East European Journal of Physics. 2. 49-54 (2025)
DOI:10.26565/2312-4334-2025-2-06 ISSN 2312-4334

EXAMINATION OF (t, ^{3}He) CHARGE EXCHANGE REACTIONS: INCORPORATING KNOCK-ON EXCHANGE AND TENSOR FORCE TERMS EFFECTS

Ankita*, Pardeep Singh**
Department of Physics, Deenbandhu Chhotu Ram University of Science and Technology, Murthal, Sonipat 131039, Haryana, India
**Corresponding Author e-mail: *ankumehra531@gmail.com; **pardeep.phy@dcrustm.org*
Received February 4, 2025; revised March 16, 2025; accepted March 20, 2025

The present study employs DWIA (Distorted Wave Impulse Approximation) framework, allows to investigate the influence of knock-on exchange effects together with tensor force contributions while examining the charge exchange reactions. Here, the differential cross-section and unit cross-section for (t, ^{3}He) charge-exchange reactions on ^{12}C, ^{13}C, ^{26}Mg and ^{58}Ni targets have been computed. The obtained results demonstrate that consideration of knock-on exchange terms substantially decreases the estimated cross-section. Furthermore, the tensor forces contribution introduces an additional layer of complexity to the analysis of charge exchange reactions. Depending on the target nucleus, the tensor forces contribution produces either constructive or destructive interference effects, which leads to either increment or decrement in cross-section magnitude based on the target nucleus. The predicted unit cross-sections agree with corresponding experimental data but show specific deviations because of tensor interactions which are most pronounced in ^{58}Ni.
Keywords: *Gamow-Teller transitions; Charge Exchange Reaction; Tensor forces; Distorted Wave Impulse Approximation; Angular Distribution; Unit cross-section*
PACS: 25.55.-e, 25.45.Kk, 25.70.Kk, 25.40.Kv

INTRODUCTION

Spin-isospin excitations within nuclei at intermediate energies have been extensively studied through hadronic probe, involving (p, n) and (^{3}He, t) charge-exchange (CE) reactions along with their inverse reactions, (n, p) and (t, ^{3}He), during the past several decades [1]-[7]. Particularly, these reactions facilitate the exchange of nucleons (protons or neutrons) between interacting nuclei such as (t, ^{3}He) reactions and same process followed by β^+- decay shown below in Figure 1, thereby inducing isospin transitions ($\Delta T = 1$) with or without associated spin-flip processes ($\Delta S = 1$ or $\Delta S = 0$). This versatility has made them particularly effective for investigating Gamow-Teller (GT) transitions, Fermi (F) transitions, and higher-order excitations such as spin-dipole and quadrupole transitions, which are often remains inaccessible through conventional beta decay [8], [9].

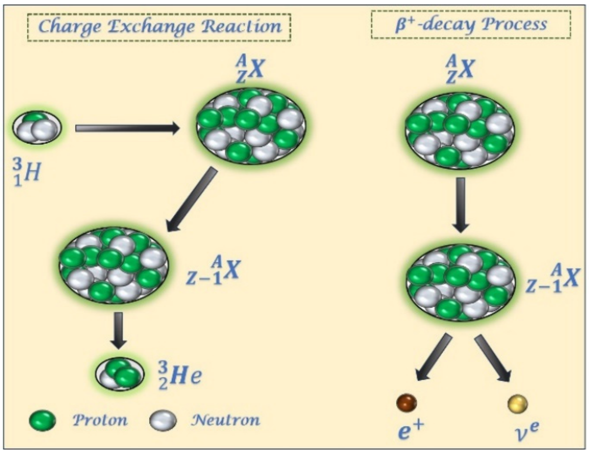

Figure 1. Illustration of (t, ^{3}He) charge exchange reaction and β^+- decay process

In recent decade, weak interaction research attracts the attention of scientists commonly around the globe, due to the fact that these processes determine fundamental explanations for nuclear physics and astrophysical phenomena. The mechanisms that control stellar evolution and initiate core-collapse supernovae remain governed by weak interaction processes. Furthermore, weak interactions play a critical role in rare nuclear processes like neutrino-less double-beta decay (0νββ), which has deep implications for understanding the nature of neutrinos and the asymmetry between matter and antimatter in the universe [10]-[13]. Additionally, weak interaction rates, particularly Gamow-Teller (GT) transition strengths characterised by changes in isospin ($\Delta T = 1$), spin ($\Delta S = 1$), and angular momentum ($\Delta L = 0$), are essential for modelling neutrino-driven nucleosynthesis pathways that contribute to the formation of heavy elements in astrophysical environments [14]-[17]. Charge exchange reactions like (t, ^{3}He) and (^{3}He, t) play a pivotal role in extracting these

Cite as: Ankita, P. Singh, East Eur. J. Phys. 2, 49 (2025), https://doi.org/10.26565/2312-4334-2025-2-06

transition strengths due to their ability to probe high-excitation energy states beyond the Q-value limitations inherent to β-decay, thereby allowing for comprehensive studies of weak interaction processes and their implications in stellar environments [18], [19]. These reactions offer high-resolution measurements, providing critical data for validating different theoretical models [20], [21].

As it is evident that at low momentum transfer, the differential cross-section measurements and GT transition strengths exhibit a well-documented proportionality, which is commonly called the unit cross-section ($\hat{\sigma}_{GT}$) [22], [23]. This relationship acts as an essential method for getting correct B(GT) values, which helps to validate theoretical models, including the shell model and quasiparticle random phase approximation (QRPA) [24]-[26]. Moreover, the experimental capabilities have been expanded through secondary triton beam developments to analyse GT strength distributions in various medium-mass nuclei [27]. Zegers et al. showed that (t, ^{3}He) along with (^{3}He, t) reactions provide effective GT probes that give matching experimental data with low probe sensitivity. The unit cross-sections $\hat{\sigma}_{GT}$ show equivalent mass dependency for nuclei having A ≥ 12, while following the relationship $\hat{\sigma}_{GT} = \frac{109}{A^{0.65}}$. This relation persists despite differences in beam energies between (t, ^{3}He) using 115 MeV/u and (^{3}He, t) using 140 MeV/u [20].

The accurate determination of Gamow-Teller strengths depends heavily on precise evaluation of knock-on exchange effects and tensor force interactions because due to approximate inclusion of these effects resulting in presence of systematic uncertainties to charge-exchange (CE) reaction results [22], [28]. However, experimental data matches more effectively with predications when antisymmetric DWIA models with precise knock-on exchange amplitudes are employed [21], [29]. Further, consideration of tensor interactions creates additional difficulties during GT strength measurements because it produces interference between the ΔL = 0 and ΔL = 2 multipoles. The interactions create systematic uncertainties reaching 20% for weak transitions [26]. Comparative studies, by Zegers et al., confirm that both (t, ^{3}He) and (^{3}He, t) reactions reliably extract Gamow-Teller (GT) strengths for weak-interaction. However, some inconsistencies arise due to consideration of higher multipole transitions (ΔL = 2) [29], systematic uncertainties from variations in optical model potentials and reaction dynamics leading to normalization discrepancies of 10–20% [14], and the pronounced impact of knock-on exchange effects requiring precise theoretical treatment for both the reaction [28].

Previously, we have examined (^{3}He, t) reaction on various targets using Distorted Wave Impulse Approximation (DWIA) at intermediate energy, wherein the importance of incorporation of knock-on exchange effects have been discussed [30]. However, in current work, we have examined (t, ^{3}He) charge exchange reaction at low and medium-mass nuclei at 140 MeV/nucleon for Gamow-Teller transitions. Both knock-on exchange effects and tensor force contributions have been incorporated to extract clearer and more precise information from these reactions.

RESULTS AND DISCUSSION

DWIA approach have been used in current work, which has been discussed in detail in refs. [30]-[32]. However, some important expressions used in calculations are discussed below. The differential cross-section may be computed by using below expression.

$$\frac{d\sigma}{d\Omega} = \frac{\mu_a \mu_b}{(2\pi\hbar^2)^2}\frac{k_b}{k_a}\left|\sum_{i=D,E}\sum_{k,l_1 t_1} \alpha_{j_t s_t v_1}^{t_1 s_1 l_1 k l_t}\, T_i^{t_1 s_1 l_1 k l_t m_{l_t}}\right|^2. \tag{1}$$

In above, μ_a *and* μ_b are the reduced mass of reactants in incoming and outgoing channel while the wave number in incident and exit channel are accounted by k_a and k_b respectively. ($\alpha_{j_t s_t v_1}^{t_1 s_1 l_1 k l_t}$) is the expansion coefficient which is further formulated in terms of Racah coefficient (W).

Currently, there is no exact method available for calculating charge-exchange reactions involving composite particles. As a result, most calculations rely on pseudo-potential approximations whose accuracy can vary significantly depending on the projectile energy and target mass. Therefore, to gain clearer insights into the influence of exchange term and tensor force terms in distorted wave impulse approximation calculations, we present results for the differential cross-section of (t, ^{3}He) reactions on ^{12}C, ^{13}C, ^{26}Mg and ^{58}Ni at a beam energy of 140 MeV/nucleon focusing on Gamow-Teller (GT) transitions. The calculated differential cross-sections are illustrated in Figure 2 (a-d) for ^{12}C, ^{13}C, ^{26}Mg and ^{58}Ni respectively. To extract the cross-section at 0°, the experimental differential cross-sections are fitted to the theoretical predictions obtained using the DWIA framework with the DCP-2 code. These calculations focus on transitions to final states with known GT strengths for the 1^+ ground state, as listed in Table 1. A key element in these calculations is the use of an effective nucleon-nucleon interaction potential (V), which plays a crucial role in accurately modelling the reaction dynamics and expressed as

$$V = \int dx_1 dx_2 dx_1' dx_2' \hat{\rho}_T(x_1 x_1')\hat{\rho}_P(x_2, x_2^1) v_{12}(x_1' x_2', x_1 x_2). \tag{2}$$

where, $x_i = (r_i, \sigma_i, \tau_i)$ stands for space, spin and iso-spin co-ordinate of i^{th} particle ($i = 1{,}2$) and x_i' co-ordinate denotes the x_i after the exchange of nucleons '1' and '2'. The interaction potential, expressed as $v_{12}(x_1' x_2', x_1 x_2) = x_1' x_2' V^D x_1 x_2 + (-)_l P^r x_1' x_2' V^E x_1 x_2$, with P^r as exchange operator, is a combination of direct and exchange part of the Love and Franey type effective interaction (V^i ($i = D$) for direct and ($i = E$) for exchange) [33], [34].

We also assume that the effective interactions contain both central and tensor terms. The tensor operator can be written as $\hat{S}_{12} = 3(\hat{\sigma}_1.\hat{r}\,)(\hat{\sigma}_2.\hat{r}\,) - (\hat{\sigma}_1.\hat{\sigma}_2\,) = \sum_q \sqrt{4\pi}\sqrt{\frac{2}{5}}\, Y^*_{2q}\hat{T}_{2q}$, where $\hat{T}_{2q}$ is a second rank tensor operator. The $\hat{\rho}_T(x_1, x_1')$ and $\hat{\rho}_P(x_2, x_2')$ respectively accounts the non-local densities for target and projectile. The value of B(GT) [14], [22] and the optical model potentials parameters (OMP) that are extracted from ^{3}He elastic scattering data are taken from refs. [35]-[38] while for outgoing channel (^{3}H) same parameters are used except potential depth which is modulated by multiplying with 0.85 [37]. The one body transition densities (OBTD's) give weight factors for each 1p-1h excitations and have been calculated using OXBASH code using sd-model space coupled with USD hamiltonian [39], while for heavier mass like ^{58}Ni, the pf-model space along with GXPF1 interactions has been used [40]. In addition, the radial wave functions used for the calculation of form factor are constructed with Woods-Saxon potential. The radial densities for the projectile (^{3}He) and ejectile (^{3}H), are obtained from Variational Monte Carlo calculations [41].

Table 1. Initial and final states of various systems excited by reaction (t, ^{3}He). B(GT) values tabulated below are calculated by employing method given in refs. [14], [22].

Initial (J^π, E)	Final (J^π, E)	B(GT)
$^{12}C(0^+, g.s.)$	$^{12}B(1^+, g.s.)$	0.99
$^{13}C(\frac{1}{2}^-, g.s.)$	$^{13}B(\frac{3}{2}^-, g.s.)$	0.711
$^{26}Mg(0^+, g.s.)$	$^{26}Na(1^+, 0.08)$	0.41
$^{58}Ni(0^+, g.s.)$	$^{58}Co(1^+, 1.87)$	0.72

Figure 2 presents the differential cross-section of (t, ^{3}He) charge exchange reaction for ^{12}C, ^{13}C, ^{18}O, ^{26}Mg, ^{58}Ni nuclei, focusing on their first Gamow-Teller (GT) states listed in Table 1.

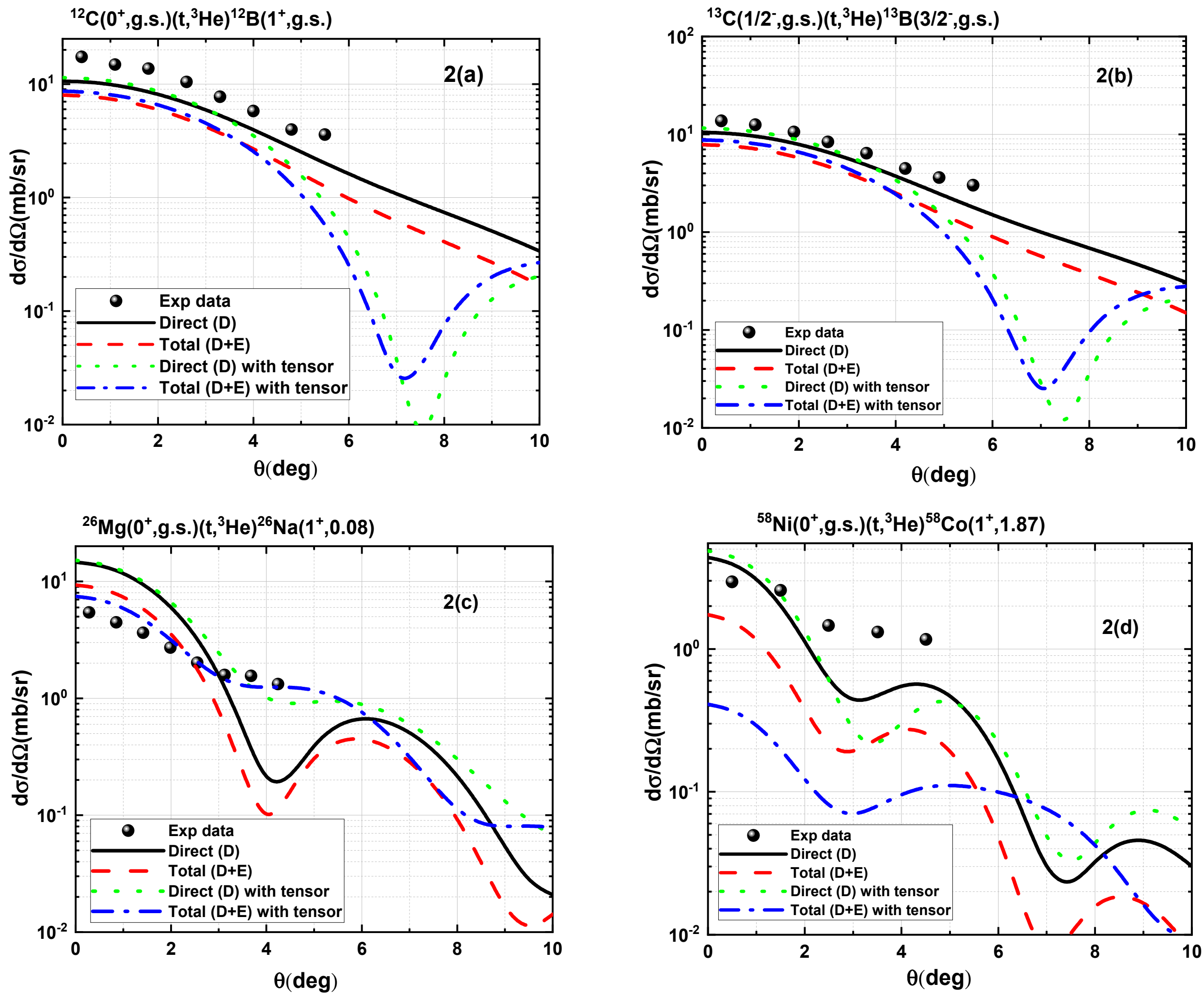

Figure 2. (Color online) The calculated differential cross-section for (t, ^{3}He) charge exchange reaction on ^{12}C, ^{13}C, ^{26}Mg and ^{58}Ni target using DWIA at 140 MeV/nucleon. The solid (black) and dashed (red) line represents the direct and total (D+E) contribution without tensor forces effect respectively. The dotted (green) and dash-dotted (blue) line represents the direct and total (D+E) contribution with tensor forces effect respectively. The solid (black) circle represents the experimentally measured data

For each target nucleus four sets of calculations were performed to evaluate the contributions of different interaction terms, (i) direct terms contributions without exchange terms calculations represented by Direct (D) (ii) direct terms with inclusion of knock-on exchange terms labelled as Total (D+E) (iii) while results obtained for tensor forces along with direct terms contribution represent are shown by Direct (D) with tensor (iv) the total contribution with tensor forces depicted by Total (D+E) with tensor. Quantitatively, the inclusion of exchange effects causes a significant reduction in the differential cross-section, in magnitudes up to 20% - 60% for all the targets considered in this work. Generally, calculations incorporating exchange terms effects, deviate from the experimental data, except for ^{26}Mg. A similar trend has been observed in earlier work performed with (^{3}He, t) reaction.

Furthermore, it is noticed that the inclusion of tensor force terms creates noticeable changes to the cross-sections, primarily in the forward scattering region. For ^{12}C and ^{13}C, the inclusion of tensor terms leads to a slight increase (up to 10%) in the differential cross-section at forward angles, constructively enhancing the cross-section and improving agreement with experimental data [22], [42]. In contrast, for ^{26}Mg and ^{58}Ni, the tensor forces interact destructively with the total (D+E) contributions. Although, for the case ^{26}Mg, tensor interference leads to a 20% reduction in the cross-section, narrowing the gap between theoretical predictions and experimental measurements [20]. For ^{58}Ni, the tensor contribution results in an even more pronounced reduction, up to 60%, which moves the theoretical predictions further away from the experimental data [14].

The variations in differential cross-sections across different nuclei can be explained by the role of the tensor component in the effective nucleon-nucleon interaction. This tensor force introduces interference between the ΔL = 0 and ΔL = 2 amplitudes, both contributing to ΔJ = 1 Gamow-Teller transitions. The nature of this interference is constructive as well as destructive, varies depending on the target nucleus and specific reaction conditions. These factors significantly influence the reaction mechanism and the degree of agreement between theoretical predictions and experimental data, depending on the target nucleus involved. To further analyze the reaction dynamics and quantify these effects, unit cross-sections have been calculated.

The unit cross-section $\hat{\sigma}_{GT}$ for charge-exchange (CE) reactions is determined using the relationship between the Gamow-Teller (GT) transition strength and the differential cross-section at zero momentum transfer, expressed as

$$\frac{d\sigma}{d\Omega}(q \to 0) = \hat{\sigma}_{GT} B(GT) \tag{3}$$

Calculating the unit cross-section typically requires known (B(GT) values, which are often obtained from β-decay measurements. In cases where such experimental data are unavailable, theoretical models must be employed to estimate the unit cross-section. Another approach involves using empirical formulas such as those presented in Ref. [20]. However, it is important to recognize that empirical methods have limited precision and theoretical calculations are generally necessary for more accurate determinations. However, we have calcuated the unit cross-section for (t, ^{3}He) charge exchange reactions and shows its variations over different target nuclei ^{12}C, ^{13}C, ^{26}Mg and ^{58}Ni.

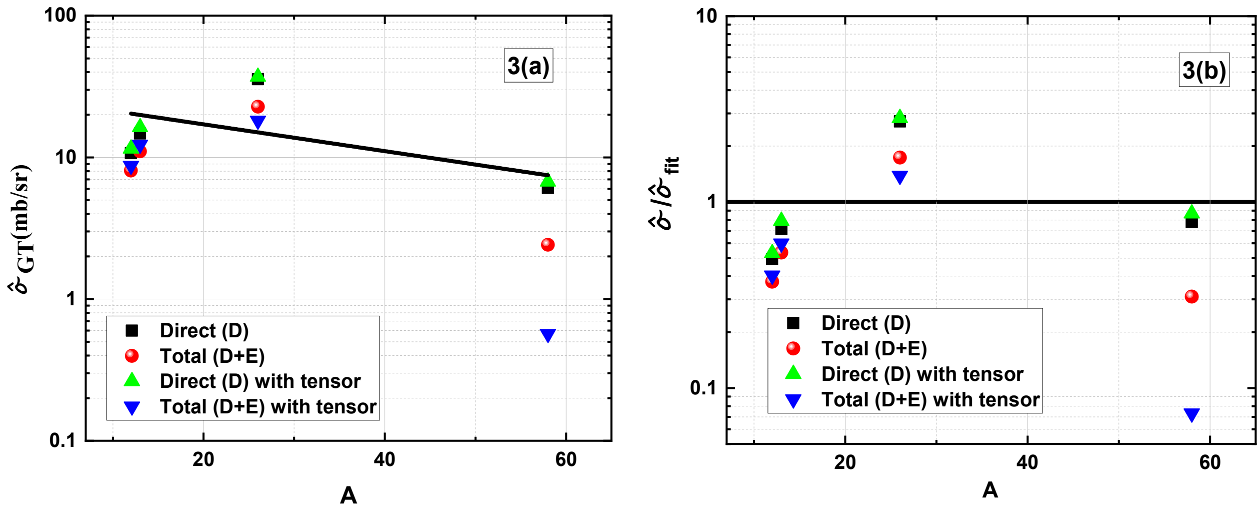

Figure 3. (Color online) (a) The calculated unit cross-section for (^{3}He, t) Charge exchange reactions on targets ^{13}C, ^{26}Mg, ^{58}Ni and ^{120}Sn for GT transitions. (b) shows the ratio of the calculated and experimental unit cross-sections relative to the fitted cross-section for Gamow-Teller transitions. In both figs., the solid square (black) and circle (red) shows direct and total (D+E) calculations without incorporating tensor forces. While upward triangle (green) and downward triangle (blue) is showing the results after consideration tensor forces in the calculation with direct and total (D+E) term respectively. The solid (black) line represents the unit cross-section obtained through fitted empirical function

Figure 3 presents four distinct calculations for each target along with the results obtained through empirical relation, $\hat{\sigma}_{GT,fit} = 109/A^{0.65}$, which is a power fit to experimental data [14]. In Figures 3 (a) and 3(b), respectively the solid square (black) and circle (red) shows direct and total (D+E) calculations without incorporating tensor forces. While upward triangle (green) and downward triangle (blue) is showing the results after consideration tensor forces in the calculation with direct and total (D+E) term respectively. The solid (black) line in the figure corresponds to the unit cross-section obtained through empirical formula. To evaluate the reliability of the conclusions drawn from the empirical relation $\hat{\sigma}_{GT,fit} = 109/A^{0.65}$, Figure 3 (b) shows the ratio of the calculated and experimental unit cross-sections relative to the fitted cross-section for Gamow-Teller transitions. This comparison helps to validate the theoretical calculations, especially in cases where experimental data is lacking.

In Figure 3 (a) it is evident that for ^{12}C, ^{13}C and ^{58}Ni nuclei, both the direct and total (D+E) calculations without tensor forces underestimate the unit cross-section predicted by the empirical fit. Conversely, for ^{26}Mg, the calculated values overestimate the empirical data. Furthermore, when tensor forces are incorporated into the direct and total (D+E) calculations, there is a noticeable reduction in the differential cross-section, by up to a factor of 2 for ^{26}Mg and up to 4 for ^{58}Ni. In contrast, for ^{12}C and ^{13}C, the inclusion of tensor forces results in only a slight increase in the cross-section magnitude compared to the results without tensor forces. Overall, the addition of tensor forces tends to align the calculated results more closely with the empirical fit for ^{12}C, ^{13}C and ^{26}Mg, improving the agreement between theory and experiment. However, for ^{58}Ni, the results further deviate from the empirical fit upon including tensor contributions. These variations arise from the behavior of the tensor component in the effective nucleon-nucleon interaction, which eventually influences the charge-exchange reaction results. Specifically, this tensor force induces interference between the $\Delta L = 0$, $\Delta S = 1$ amplitudes (mediated by the $\sigma\tau$ component) and the $\Delta L = 2$, $\Delta S = 1$ amplitudes (mediated by the tensor-τ component). Since both of these transitions contribute to the $\Delta J = 1$ Gamow-Teller transitions, the nature of the interference can be either constructive or destructive, depending on the specific nuclear system and reaction conditions.

SUMMARY AND CONCLUSION

In this work, (t, ^{3}He) charge-exchange reactions at 140 MeV/nucleon on ^{12}C, ^{13}C, ^{26}Mg and ^{58}Ni targets have been examined. Differential cross-sections and unit cross-sections have been computed by incorporating both knock-on exchange effects and tensor force components through DWIA approach with computer code DCP-2. Calculations shows that knock-on exchange effects reduced the predicted cross-sections by 20% - 60%. Further, it has been also noticed that the incorporation of exchange terms produces better predictions of experimental results for ^{26}Mg nuclei. It is worth to mention here that the inclusion of tensor force terms produces intricate patterns of destructive and constructive interference between the $\Delta L = 0$ and $\Delta L = 2$ components. The destructive interference has been noticed in case of ^{26}Mg and ^{58}Ni which eventually causes to reduction cross-sections up to 60%. A good agreement between calculated unit cross-sections and experimental data has been found for all the targets considered here except ^{58}Ni.

In conclusion, the study establishes fundamental understanding of (t, ^{3}He) process behavior while demonstrating the requirement of considering advanced nuclear interactions for achieving accurate theoretical predictions.

Acknowledgment

The First author would like to acknowledge University Grant Commission (UGC) for providing the fellowship vide Ref. No. 19/06/2016(i)EU-V.

ORCID

Ankita, https://orcid.org/0000-0001-5769-2907; **Pardeep Singh,** https://orcid.org/0000-0003-2100-3772

REFERENCES

[1] T.N. Taddeucci, et al., Nucl. Phys. A **469**, 125 (1987), https://doi.org/10.1016/0375-9474(87)90089-3
[2] M.N. Harakeh, and A.V. Woude, *Giant Resonances: Fundamental High Frequency Modes of Nuclear Excitations*, (Oxford University, New York, 2001).
[3] B. Gao, et al., Phys. Rev. C **101**, 014308 (2020), https://doi.org/10.1103/PhysRevC.101.014308
[4] J. J. Li, et al., Phys. Rev. C **102**, 064601 (2020), https://doi.org/10.1103/PhysRevC.102.064601
[5] Y. Fujita, et al., Phys. Rev. C **67**, 064312 (2003), https://doi.org/10.1103/PhysRevC.67.064312
[6] B. T. Kim, et al., Phys. Rev. C **61**, 044611 (2000), https://doi.org/10.1103/PhysRevC.61.044611
[7] D. T. Khoa, et al., Phys. Rev. C **76**, 014603 (2007), https://doi.org/10.1103/PhysRevC.76.014603
[8] D. Vale, et al., Phys. Rev. C **103**, 064307 (2021), https://doi.org/10.1103/PhysRevC.103.064307
[9] D. Gambacurta, et al., Phys. Rev. Lett. **125**, 212501 (2020), https://doi.org/10.1103/PhysRevLett.125.212501
[10] F. T. Avignone, et al., Rev. Mod. Phys. **80**, 481 (2008), https://doi.org/10.1103/RevModPhys.80.481
[11] J. Engel, et al., Rep. Prog. Phys. **80**, 046301 (2017), https://doi.org/10.1088/1361-6633/aa5bc5
[12] J. Menendez, et al., J. Phys. G **45**, 014003 (2017), https://doi.org/10.1088/1361-6471/aa9bd4
[13] F. Cappuzzello, et al., Prog. Part. Nucl. Phys. **128**, 103999 (2023), https://doi.org/10.1016/j.ppnp.2022.103999
[14] A. L. Cole, et al., Phys. Rev. C **74**, 034333 (2006), https://doi.org/10.1103/PhysRevC.74.034333
[15] Y. Fujita, et al., Phys. Rev. C **70**, 011306(R) (2004), https://doi.org/10.1103/PhysRevC.70.011306
[16] F. Diel, et al., Phys. Rev. C **99**, 054322 (2019). https://doi.org/10.1103/PhysRevC.99.054322
[17] H. Fujita, et al., Phys. Rev. C **100**, 034618 (2019), https://doi.org/10.1103/PhysRevC.100.034618
[18] J. C. Zamora, et al., Phys. Rev. C **100**, 032801 (2019), https://doi.org/10.1103/PhysRevC.100.032801
[19] S. Noji, et al., Phys. Rev. C **92**, 024312 (2015), https://doi.org/10.1103/PhysRevC.92.024312
[20] R.G.T. Zegers, et al., Phys. Rev. C **74**, 024309 (2006), https://doi.org/10.1103/PhysRevC.74.024309

[21] T. Udagawa, A. Schulte, and F. Osterfeld, Nucl. Phys. A, **474**, 131 (1987). https://doi.org/10.1016/0375-9474(87)90197-7
[22] G. Perdikakis, *et al*., Phys. Rev. C, **83**, 054614 (2011). https://doi.org/10.1103/PhysRevC.83.054614
[23] R.G.T. Zegers, *et al*., Phys. Rev. Letts. **99**, 202501 (2007). https://doi.org/10.1103/PhysRevLett.99.202501
[24] R. Titus, *et al*., J. Phys. G: Nucl. Part. Phys. **45**, 014004 (2017). https://doi.org/10.1088/1361-6471/aa98c1
[25] R. Titus, *et al*., Phys. Rev. C, **100**, 045805 (2019). https://doi.org/10.1103/PhysRevC.100.045805
[26] A. L. Cole, *et al*., Phys. Rev. C, **86**, 015809 (2012). https://doi.org/10.1103/PhysRevC.86.015809
[27] G.W. Hitt, *et al*., Nuclear Instruments and Methods in Physics Research A **566**, 264 (2006). https://doi.org/10.1016/j.nima.2006.07.045
[28] B. T. Kim, *et al*., Phys. Rev. C, **61**, 044611 (2000). https://doi.org/10.1103/PhysRevC.61.044611
[29] A. Schulte, e*t al*., Phys. Lett. B, **183**, 243 (1987). https://doi.org/10.1016/0370-2693(87)90956-7
[30] Ankita, and P. Singh, Mod. Phys. Lett. A, **38**, 2350066 (2023). https://doi.org/10.1142/S0217732323500669
[31] Riken, https://www.nishina.riken.jp/researcher/archive/program., Nishina center for accelerator-based science.
[32] P. Singh, *et al*., Mod. Phys. Lett. A, **35**, 2020045 (2020). https://doi.org/10.1142/S0217732320500455
[33] W.G. Love, and M.A. Franey, *et al*., Phys. Rev. C, **24**, 1073 (1981). https://doi.org/10.1103/PhysRevC.24.1073
[34] M.A. Franey, and W.G. Love, *et al*., Phys. Rev. C, **31**, 488 (1985). https://doi.org/10.1103/PhysRevC.31.488
[35] H. Fujimura, et al., Phys. Rev. C **69**, 064327 (2004). https://doi.org/10.1103/PhysRevC.69.064327
[36] T. Yamagata, et al., Nucl. Phys. A **589**, 425 (1995). https://doi.org/10.1016/0375-9474(95)00071-8
[37] S. Y. Van Der Werf et al., Nucl. Phys. A **496**, 305 (1989). https://doi.org/10.1016/0375-9474(89)90177-2
[38] J. Kamiya, et al., Phys. Rev. C, **67**, 064612 (2003). https://doi.org/10.1103/PhysRevC.67.064612
[39] M. Honma, *et al*., Phys. Rev. C, **69**, 034335 (2004). https://doi.org/10.1103/PhysRevC.69.034335
[40] C.A. Douma, *et al*., Eur. Phys. J. A, **56**, 51 (2020). https://doi.org/10.1140/epja/s10050-020-00044-9
[41] S.C. Pieper, *et al*., Annu. Rev. Nucl. Part. Sci. **51**, 53 (2001). https://doi.org/10.1146/annurev.nucl.51.101701.132506
[42] C.J. Guess, *et al*., Phys. Rev. C, **80**, 024305 (2009). https://doi.org/10.1103/PhysRevC.80.024305

ДОСЛІДЖЕННЯ РЕАКЦІЙ ОБМІНУ ЗАРЯДУ (t, ^{3}He): ВРАХУВАННЯ ЧЛЕНІВ ОБМІНУ ВИБИВАННЯМ ТА ТЕНЗОРНОЇ СИЛИ

Анкіта, Пардіп Сінгх
Фізичний факультет, Університет науки та технологій імені Дінбандху Чхоту Рама, Муртал, Соніпат 131039, Харьяна, Індія

У цьому дослідженні використовується структура DWIA (Distorted Wave Impulse Approximation), яка дозволяє досліджувати вплив ефектів обміну вибиванням разом із внесками тензорної сили під час дослідження реакцій обміну зарядом. Тут було обчислено диференціальний переріз і одиничний переріз для (t, ^{3}He) реакцій обміну зарядом на мішенях ^{12}C, ^{13}C, ^{26}Mg і ^{58}Ni. Отримані результати демонструють, що врахування умов обміну суттєво зменшує розрахунковий переріз. Крім того, внесок тензорних сил вносить додатковий рівень складності в аналіз реакцій обміну зарядом. Залежно від цільового ядра, внесок тензорних сил створює або конструктивні, або деструктивні ефекти інтерференції, що призводить або до збільшення, або до зменшення величини поперечного перерізу на основі цільового ядра. Прогнозовані одиничні перерізи узгоджуються з відповідними експериментальними даними, але демонструють специфічні відхилення через тензорні взаємодії, які найбільш виражені в ^{58}Ni.

Ключові слова: *переходи Гамова-Теллера; реакція обміну заряду; тензорні сили; апроксимація спотвореного хвильового імпульсу; кутовий розподіл; поперечний переріз*